Bull Volcanol (2013) 75:746
DOI 10.1007/s00445-013-0746-x

RESEARCH ARTICLE

Origin of fumarolic fluids from Tupungatito Volcano (Central Chile): interplay between magmatic, hydrothermal, and shallow meteoric sources

Oscar Benavente · Franco Tassi · Francisco Gutiérrez · Orlando Vaselli · Felipe Aguilera · Martin Reich

Received: 7 March 2013 / Accepted: 28 June 2013 / Published online: 25 July 2013

Abstract Tupungatito is a poorly known volcano located about 100 km eastward of Santiago (Chile) in the northernmost sector of the South Volcanic Zone. This 5,682 m high volcano shows intense fumarolic activity. It hosts three crater lakes within the northwestern portion of the summit area. Chemical compositions of fumarolic gases and isotopic signatures of noble gases ($^3He/^4He$ and $^{40}Ar/^{36}Ar$ are up to 6.09 Ra and 461, respectively), and steam ($\delta^{18}O$ and δD) suggest that they are produced by mixing of fluids from a magmatic source rich in acidic gas compounds (SO_2, HCl, and HF), and meteoric water. The magmatic–hydrothermal fluids are affected by steam condensation that controls the outlet fumarolic temperatures (<83.6 °C), the gas chemical composition, and the steam isotopic values. The $\delta^{13}C–CO_2$ values (ranging from 0.30 and −8.16‰ vs. V-PDB) suggest that CO_2 mainly derives from (1) a mantle source likely affected by significant contamination from the subducting slab, (2) the sedimentary basement, and (3) limited contribution from crustal sediments. Gas geothermometry based on the kinetically rapid $H_2–CO$ equilibria indicates equilibrium temperatures <200 °C attained in a single vapor phase at redox conditions slightly more oxidizing than those commonly characterizing hydrothermal reservoirs. Reactions in the $H_2O–CO_2–H_2–CO–CH_4$ system and $C_2–C_3$ alkenes/alkanes pairs, which have relatively slow kinetics, seem to equilibrate at greater depth, where temperatures are >200 °C and redox conditions are consistent with those inferred by the presence of the $SO_2–H_2S$ redox pair, typical of fluids that have attained equilibrium in magmatic environment. A comprehensive conceptual geochemical model describing the circulation pattern of the Tupungatito hydrothermal–magmatic fluids is proposed. It includes fluid source regions and re-equilibration processes affecting the different gas species due to changing chemical–physical conditions as the magmatic–hydrothermal fluids rise up toward the surface.

Keywords Fumarolic fluid · Tupungatito volcano · Fluid geochemistry · Southern Volcanic Zone

Editorial responsibility: P. Wallace

O. Benavente (✉) · F. Gutiérrez · M. Reich
Departamento de Geología, Universidad de Chile, Plaza Ercilla 803, 8370450 Santiago, Chile
e-mail: obenaven@ing.uchile.cl

O. Benavente · F. Gutiérrez · F. Aguilera · M. Reich
Centro de Excelencia en Geotermia de los Andes (CEGA), Universidad de Chile, Plaza Ercilla, 803, 8370450 Santiago, Chile

F. Tassi · O. Vaselli
Dipartimento di Scienze della Terra, Università degli Studi di Firenze, Via G. La Pira, 4, 50121 Florence, Italy

F. Tassi · O. Vaselli
CNR-IGG Istituto di Geoscienze e Georisorse, Università degli Studi di Firenze, Via G. La Pira, 4, 50121 Florence, Italy

F. Aguilera
Departamento de Geología, Universidad de Atacama, Copayapu 485, 1532296 Copiapó, Chile

Introduction

The chemical and isotopic compositions of fluids naturally discharged into the atmosphere from volcanic systems are the result of the interplay between (1) deep processes, e.g., vapor–melt separation, and(2) secondary processes that include gas cooling and re-equilibration, interaction with meteoric water-fed aquifers, reactions with wall rock minerals, microbial activity, and air contamination (Giggenbach 1980, 1984, 1987, 1988, 1996; Chiodini and Marini 1998; Capaccioni and Mangani 2001; Symonds et al. 2001; Taran and Giggenbach 2003). Geochemical investigations of fumarolic fluids from volcanic systems are commonly aimed at reconstructing fluid sources and chemical–physical conditions occurring along the fluid circulation pattern to serve as a basis

for monitoring purposes and/or evaluation of geothermal energy potential (e.g., Tedesco and Sabroux 1987; Martini et al. 1991; Giggenbach 1996; Tassi et al. 2005a, b; Sepúlveda et al. 2007; Vaselli et al. 2010).

Tupungatito is an early Pleistocene–Holocene volcano located ~100 km east of Santiago in the High Andes of Central Chile (Fig. 1a) in the northernmost sector of the South Volcanic Zone (SVZ). This volcano is characterized by a permanent fumarolic activity and the occurrence of three crater lakes at its summit showing intense gas bubbling (González-Ferrán 1995). To the best of our knowledge, no geochemical data for these volcanic fluids are currently available. In this study, we present and discuss the very first chemical and isotopic ($\delta^{13}C$–CO_2, $^3He/^4He$, and $^{40}Ar/^{36}Ar$) data on the composition of fumarolic gases and steam ($\delta^{18}O$ and δD), as well as the chemical composition of the lake hosted in the 1986–1987 summit crater (Fig. 1c), using samples collected from this Chilean volcano during two campaigns carried out in February 2011 and 2012. The main aims were to investigate the different fluid source regions

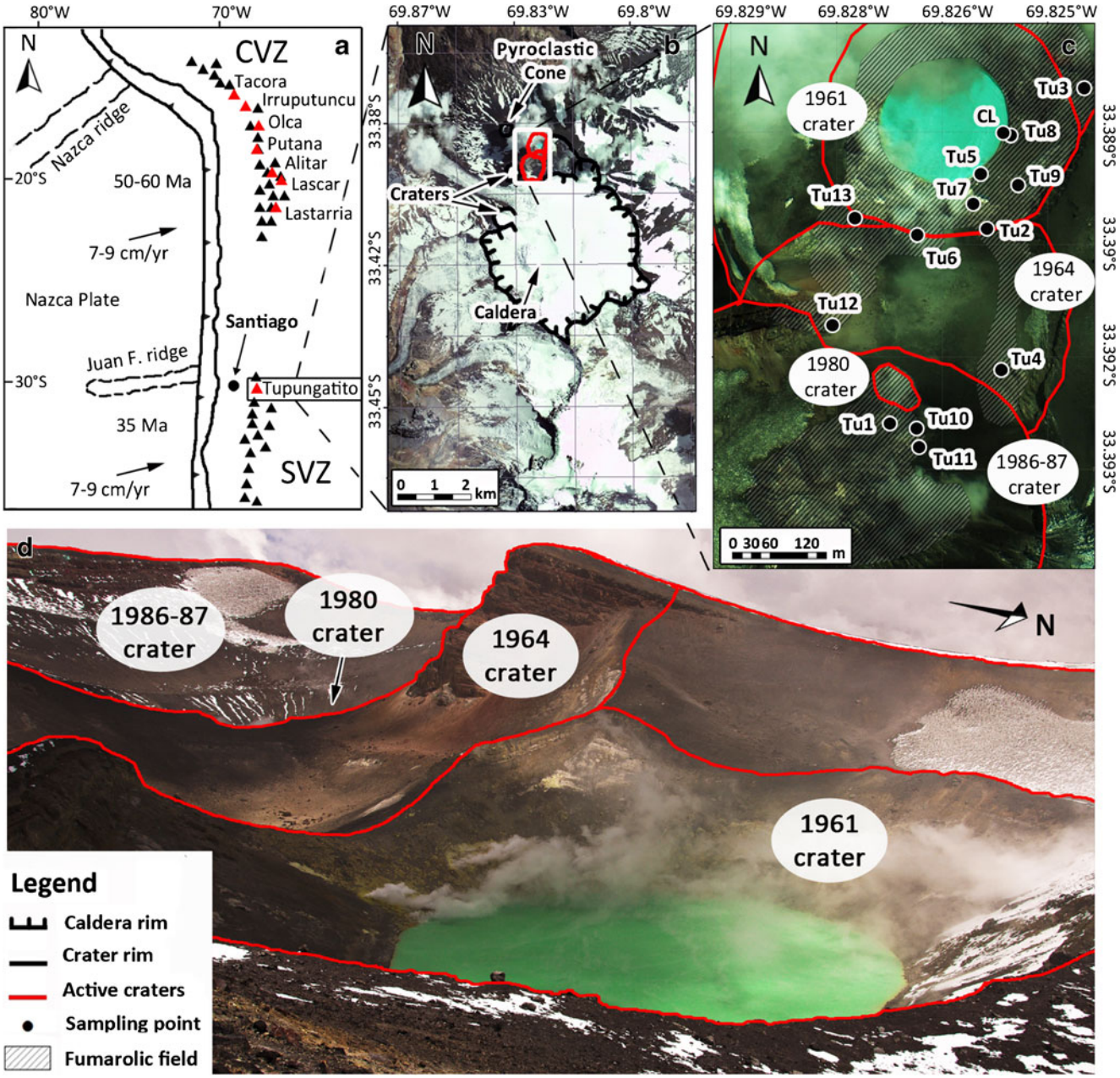

Fig. 1 **a** Location of the Tupungatito volcano and active and dormant volcanic centers of the Central and Southern Volcanic Zones; **b** aerial image of Tupungatito and Tupungato volcanic complex; **c** summit actives crater of Tupungatito volcano, showing the locations of the fumarolic fields and sampling sites; **d** view from SW of the three main active craters in the Tupungatito summit

and the chemical–physical processes controlling fluid chemistry. These geochemical data are compared with those of fumarolic fluids from other volcanic systems located in the Chilean Andes (Fig. 1a) that are characterized by different (1) amount and composition of the subducted sediment, (2) slab thermal state, and (3) crustal thickness and lithology.

Geodynamic, geological, and volcanological settings

Volcanism in the Andes of Chile is produced by the subduction of the Nazca and Antarctic plates below the South America plate (Barazangi and Isacks 1976; Cande and Leslie 1986, 1987). The Chilean Volcanic Chain consists of three distinct volcanic alignments characterized by a relatively steep subduction angle (>25°): Central (CVZ; 17.5–27°S), Southern (SVZ; 33–46°S) and Austral (AVZ; 49–55°S) Volcanic Zones (Fig. 1a; Barazangi and Isacks 1976).

Tupungatito volcano (33.4°S, 69.8°W; 5682 m above sea level (a.s.l.)) consists of (1) seven summit craters, (2) a northwesternmost 4-km wide pyroclastic cone, and (3) a 5-km wide caldera with an estimated erupted volume of 6 km^3 that opens westwards (Fig. 1b; Hildreth and Moorbath 1988; González-Ferrán 1995; Moreno and Naranjo 1991). The caldera is covered by glaciers above 5,400 m a.s.l., where the ice melt waters are discharged into the Colorado–Maipo drainage basin to the west (Fig. 1b; Stern et al. 2007). The base of the volcanic edifice (4,700 m a.s.l.) overlies an eroded volcano whose estimated volume is >10 km^3 and consists of dacitic lavas and lithic pyroclastic flows lithologically similar to those of Tupungato stratovolcano (6,550 m a.s.l.), which is located 7 km NW of Tupungatito (Hildreth and Moorbath 1988). The sedimentary basement of the Tupungatito volcano is composed of thick Lower Cretaceous marine limestone and evaporitic sequences (Giambiagi and Ramos 2002). Upper Cretaceous conglomerate and sandstone beds, and volcanoclastic rocks overlay the Lower Cretaceous sequences, and outcrop ~10 km west from the volcano (Giambiagi and Ramos 2002). In this area, the crustal thickness is ~50 km (Barazangi and Isacks 1976; Tassara and Yáñez 2003). The Tupungatito eruptive products range from basaltic–andesites to dacites (Hildreth and Moorbath 1988). Compared to the volcanic rocks of the southern portions of the SVZ, where crustal thickness progressively decreases down to 30 km (Barazangi and Isacks 1976; Tassara and Yáñez 2003), the Tupungatito magmas, at equivalent SiO_2 contents (~57.5 %), has higher contents of K_2O (~2.82 %) and incompatible trace elements (Rb ~80 ppm, Sr ~600 ppm, Ba ~520 ppm, and Th ~9 ppm), higher ratios of fluid-mobile elements (Ce/Yb ~45 and Rb/Cs ~30), higher $^{87}Sr/^{86}Sr$ isotope ratios (0.70489), and lower K/Rb and $^{143}Nd/^{144}Nd$ ratios (~250 and 0.511589, respectively; Hildreth and Moorbath 1988). The crustal signature of the Tupungatito volcanic products was interpreted by Cembrano and Lara (2009) in terms of advanced magmatic differentiation related to long residence times in the crust of magmas, as they were rising through a thick crust in a compressive tectonic regime.

Tupungatito volcano is one of the most active volcanoes in the SVZ, having experienced 19 historical eruptions between 1829 and 1987 (Moreno and Naranjo 1991; González-Ferrán 1995). Historical eruptions were characterized by a VEI <2 and occurred in the NW portion of the caldera, where eight active craters were formed (Fig. 1c; González-Ferrán 1995). Currently, four NS-oriented summit craters are characterized by permanent fumarolic activity and host three crater lakes (Fig. 1c, d), which show a vigorous gas bubbling. The turquoise-colored crater lake, hosted in the northernmost active crater formed in 1961 (Fig. 1c, d; González-Ferrán 1995), has an extremely low pH (<1), caused by dissolution of acidic gases. Fumaroles were also recognized along the eastern and western rims of the central crater that was produced by an explosive eruption that occurred in 1964 (Fig. 1c; González-Ferrán 1995). The last three eruptions (1980, 1986, and 1987), mainly consisting of phreatic activity, occurred in the third crater (Fig. 1c; Moreno and Naranjo 1991; González-Ferrán 1995), which hosts two inaccessible small crater lakes located at the bottom of the 1980 and 1986–1987 craters and several fumarolic vents (Fig. 1c).

Sampling and analytical methods

Gas and water sampling

Gas samples from fumarolic vents and bubbling pools were collected using pre-evacuated 60-mL glass Giggenbach-like (Giggenbach 1975) flasks filled with 20 mL of 4 N NaOH and a 0.15 M $Cd(OH)_2$ suspension (Montegrossi et al. 2001; Vaselli et al. 2006). Gas samples from fumarolic vents were conveyed into the sampling flasks using a 1-m long titanium tube ($\varnothing$=2.5 cm) that was inserted into the fumarolic vent and connected through glass Dewar tubes. A gas sample from one of the many bubbling emissions in the northernmost crater lake was also collected using a plastic funnel upside-down positioned and connected to the sampling flasks through Tygon tubes. At each sampling point, a 60-mL glass pre-evacuated gas vial was used to collect a sample for the analysis of carbon isotopes in CO_2 using the same sampling apparatus adopted for the soda flasks. Fumarolic condensates were collected using an ice-cooled glass condensing system connected to the gas sampling glass line. A filtered (at 0.45 μm) water sample was collected from the crater lake and stored in 200-mL sterile polyethylene bottles.

Chemical and isotopic (R/Ra, $\delta^{13}C–CO_2$ and $^{40}Ar/^{36}Ar$) analysis of gases and steam ($\delta^{18}O$ and δD)

Inorganic gases (N_2, O_2, H_2, He, Ar, CO, and Ne) in the sampling flask headspace were analyzed using a Shimadzu 15A gas chromatograph (GC) equipped with a 10 m long 5A molecular sieve column and a thermal conductivity detector. To allow a complete separation of Ar and O_2 peaks, the oven temperature was lowered to −10 °C by means of a cryogenic liquid CO_2 cooling loop (Shimadzu CRG-15). Hydrocarbons, including CH_4, were determined by using a Shimadzu 14A GC equipped with a 10-m-long stainless steel column packed with Chromosorb PAW 80/100 mesh coated with 23 % SP 1700 and a flame ionization detector. The alkaline suspension was centrifuged at 4,000 rpm for 30 min to separate the solid precipitate from the solution. The latter was used to analyze (1) CO_2, as CO_3^{2-}, by titration (Metrohm Basic Titrino) with a 0.5 N HCl solution; (2) HCl, as Cl^-, by ion chromatography (IC; Metrohm Basic761); (3) SO_2, as SO_4^{2-}, after oxidation with 5 ml H_2O_2 (33 %) by ion chromatography. Using 5 ml H_2O_2 (33 %), CdS in the solid precipitate was oxidized to SO_4^{2-} that was analyzed by IC for determining H_2S concentrations (Montegrossi et al. 2001). Condensate samples for F^- and Cl^- were also analyzed by IC. HF concentrations were calculated on the basis of F^- and Cl^- concentrations in the condensate samples and the alkaline solution samples. The analytical error for titration, GC, and IC analyses is <5 %.

The analysis of $^{13}C/^{12}C$ ratios of CO_2 (hereafter expressed as $\delta^{13}C–CO_2$‰ vs. V-PDB) stored in the pre-evacuated sampling flasks were carried out with a Finningan Delta S mass spectrometer after standard extraction and purification procedures of the gas mixtures (Evans et al. 1998; Vaselli et al. 2006). Internal (Carrara and San Vincenzo marbles) and international (NBS18 and NBS19) standards were used for estimation of external precision. The analytical error and the reproducibility were ±0.05 and ±0.1‰, respectively.

Helium (expressed as R/Ra, where R is the $^3He/^4He$ measured ratio and Ra is the $^3He/^4He$ ratio in the air; 1.39×10^{-6}; Mamyrin and Tolstikhin 1984) and argon ($^{40}Ar/^{36}Ar$) isotopic ratios were determined on gas aliquots transferred from the flask headspace into pre-evacuated 50-mL flasks. A double collector mass spectrometer (VG 5400-TFT) was used according to the method described by Inguaggiato and Rizzo (2004). The analytical uncertainty for the determination of R/Ra and $^{40}Ar/^{36}Ar$ was ≤0.3 %.

The $^{18}O/^{16}O$ and $^2H/^1H$ isotopic ratios of the condensate samples (hereafter expressed as $\delta^{18}O–H_2O$ and $\delta D–H_2O$‰ vs. V-SMOW, respectively) were analyzed using a Finningan Delta Plus XL mass spectrometer at the Geokarst Engineering Laboratory (Trieste, Italy). Oxygen isotopes were analyzed according to the method described by Epstein and Mayeda (1953). Hydrogen isotopes were analyzed on H_2 generated by the reaction of 10 μL water with metallic zinc at 500 °C according to the analytical procedure described by Coleman et al. (1982). V-SMOW and SLAP were used as analytical standards and AR-1 as an internal standard. The analytical error is ±0.1‰ for $\delta^{18}O$ and ±0.1‰ for δD.

Chemical analysis of water

Temperature and pH of lake water were measured in situ. Major cations (Na^+, K^+, Ca^{2+}, Mg^{2+}, and NH_4^+) and anions (F^-, Cl^- SO_4^{2-}, and Br^-) of the lake water sample collected from the 1961 crater were analyzed by ion chromatography (Metrohm 861 and Metrohm 761, respectively). The analytical error for IC is ≤5 %.

Results

Chemical composition of gases

The measured temperatures of the fumaroles at Tupungatito are between 81 and 84 °C (Table 1). Steam is the main fumarolic component, while the dry gas fraction, whose molar concentration ranges from 18.5 to 27.7 %, is dominated by CO_2 (up to 980 mmol/mol) and has relatively high concentrations of H_2S (up to 25 mmol/mol), and low but detectable concentrations of acidic components, such as HCl (up to 0.31 mmol/mol), SO_2 (up to 0.248 mmol/mol), and HF (0.026 mmol/mol). Nitrogen (up to 5.187 mmol/mol) and H_2 (up to 2.61 mmol/mol) constitute a significant portion of the dry gas fraction, whereas CH_4, O_2, Ar, CO, and He have concentrations up to 0.439, 0.028, 0.0066, 0.0024, and 0.0009 mmol/mol, respectively (Table 1). The sum of the light hydrocarbons (C_2–C_7) is ≤2.9 μmol/mol (Table 2).

The chemical composition of the gas sample collected from the lake (Tu8) is similar to that of the fumaroles (Tables 1 and 2), with the exception of CO concentration, which is below the detection limit (<0.005 mmol/mol; Table 1).

Isotopic composition of gases (R/Ra, $\delta^{13}C–CO_2$, $^{40}Ar/^{36}Ar$) and steam ($\delta^{18}O$ and δD)

The isotopic compositions of water vapor ($\delta^{18}O–H_2O$ and $\delta D–H_2O$), CO_2 ($\delta^{13}C–CO_2$), He (R/R_a), and Ar ($^{40}Ar/^{36}Ar$) isotopic ratios are reported in Table 3. The $\delta^{18}O$ and δD values range from −3.3 to 0.8 and from −75 to −50‰ vs. V-SMOW, respectively. The $\delta^{13}C–CO_2$ values, with the exception of that of sample Tu8 (−0.30‰ vs. V-PDB), are from −8.16 to −5.31‰ vs. V-PDB, i.e., in the range of mantle-type CO_2 (Taylor 1986). The R/R_a values range from 5.06 to 6.09, while the $^{40}Ar/^{36}Ar$ ratios are up to 461.

Table 1 Geographical coordinates (UTM), altitude (in meter), type, outlet temperatures (in degree Celsius), and chemical composition of inorganic gases and CH_4 (in millimole per mole) for the Tupungatito gas discharges

	Date	Coord N	Coord E	Altitude	T (°C)	CO_2	HCl	HF	SO_2	H_2S	N_2	CH_4	Ar	O_2	H_2	He	CO	*X*gas %
Tu1	14 Feb. 2011	6304903	423082	5,236	83.1	970	0.058	0.0060	0.11	19	4.6	0.44	0.0040	0.018	2.4	0.0008	0.0019	27.4
Tu2	14 Feb. 2011	6305161	423203	5,233	82.4	970	0.095	0.0080	0.098	20	4.1	0.31	0.0040	0.019	2.0	0.0006	0.0015	24.3
Tu3	14 Feb. 2011	6305359	423316	5,261	83.0	970	0.085	0.0069	0.17	20	4.2	0.29	0.0057	0.029	2.2	0.0009	0.0017	27.7
Tu4	14 Feb. 2011	6304982	423211	5,267	82.7	970	0.11	0.0076	0.19	22	4.6	0.40	0.0031	0.0046	2.4	0.0008	0.0016	26.3
Tu5	14 Feb. 2011	6305245	423198	5,190	82.7	970	0.31	0.026	0.21	20	4.9	0.33	0.0039	0.0081	2.2	0.0008	0.0019	27.5
Tu6	16 Feb. 2012	6305149	423117	5,235	83.0	980	0.048	0.0051	0.23	14	4.2	0.23	0.0038	0.011	2.0	0.0006	0.0015	21.8
Tu7	16 Feb. 2012	6305199	423192	5,204	83.4	980	0.091	0.0089	0.25	12	4.7	0.31	0.0045	0.0093	2.6	0.0008	0.0022	20.9
Tu8	17 Feb. 2012	6305292	423220	5,204	35.2	980	0.051	0.0023	n.r.	11	9.0	0.22	0.032	0.044	0.37	0.001	n.r.	
Tu9	17 Feb. 2012	6305234	423235	5,222	83.5	980	0.098	0.0056	0.22	12	5.2	0.19	0.0061	0.011	1.2	0.0006	0.0016	25.6
Tu10	19 Feb. 2012	6304896	423115	5,265	83.4	970	0.086	0.0077	0.17	20	5.1	0.36	0.0066	0.012	1.9	0.0007	0.0021	24.7
Tu11	19 Feb. 2012	6304879	423116	5,258	83.6	970	0.075	0.0026	0.16	25	4.7	0.39	0.0047	0.0089	1.7	0.0005	0.0015	18.5
Tu12	20 Feb. 2012	6305032	423006	5,276	82.7	980	0.022	0.0018	0.14	16	4.7	0.42	0.0058	0.0087	0.80	0.0006	0.0006	18.8
Tu13	20 Feb. 2012	6305178	423033	5,258	80.8	980	0.031	0.0019	0.085	16	4.1	0.36	0.0064	0.0087	1.8	0.0007	0.0024	19.4

b.d.l. below detection limit

Chemical composition of water

Temperature, pH, and chemical composition of the crater lake are reported in Table 4. Temperature and pH are 32.2 and 0.34 °C, respectively. The lake chemistry is dominated by SO_4^{2-} and Cl^- (12,600 and 12,500 mg/L, respectively), whereas Ca^{2+} is the most abundant cation (1,100 mg/L), followed by Na^+ (590 mg/L), K^+ (360 mg/L), and Mg^{2+} (310 mg/L). The concentrations of NH_4^+, F^-, and Br^- are relatively high (240, 210, and 21 mg/L, respectively).

Discussion

Crater lake chemistry

The hyperacid lake hosted in the 1961 summit crater shows compositional features typical of volcanic lakes acting as condensers and calorimeters for acid volatiles and heat released from hydrothermal–magmatic degassing (Brantley et al. 1993). Fumarolic gases bubbling in the lake partially dissolve, producing high concentrations of F^-, Cl^-, SO_4^{2-}, and NH_4^+, relatively high water temperature and extremely low pH values (Table 4). Water–rock interactions, which are favored at low pH, explain the relatively high Ca^{2+}, Na^+, K^+, and Mg^{2+} concentrations (Table 4). According to the classification based on the main physical–chemical parameters proposed by Pasternack and Varekamp (1997) and Varekamp et al. (2000), the Tupungatito lake can be defined as a "high-activity lake", similar to those of other active volcanic systems, such as Ruapheu (New Zealand; Christenson and Wood 1993), Kawah (Indonesia; Delmelle et al. 2000), Poàs and Rincon de la Vieja (Costa Rica; Tassi et al. 2009b), and Copahue (Argentina; Varekamp et al. 2006).

Chemical–physical conditions at the fluid source

Chemical–physical conditions of hydrothermal–magmatic fluid reservoirs can be investigated by applying techniques developed for the interpretation of gas compositions regulated by gas–gas and gas–rock reactions that at increasing temperatures tend to approach equilibrium (Giggenbach 1987, 1993, 1996, 1997; Chiodini and Marini 1998; Taran and Giggenbach 2003). The log-ratio between the molar concentrations of H_2 and H_2O (R_H) is considered the most suitable parameter for describing the redox state of volcanic fluids (Giggenbach 1987). The temperature-independent $FeO–FeO_{1.5}$ redox pair, which is considered the most reliable redox buffer for hydrothermal systems, produces a R_H of −2.8, whereas in a magmatic gas-dominated environment the $SO_2–H_2S$ redox pair causes, at temperatures <700 °C, more oxidizing conditions (R_H<−2.8; Giggenbach 1987).

Table 2 C_2–C_7 hydrocarbons contents (in millimole per mole) for the Tupungatito gas discharges

	C_2H_6	C_2H_4	C_3H_8	C_3H_6	i-C_4H_{10}	n-C_4H_{10}	i-C_4H_8	C_4H_4O	C_6H_6	C_4H_4S	C_7H_8
Tu1	2.0	0.0033	0.14	0.0032	0.0047	0.010	0.085	0.000030	0.26	0.00060	0.0013
Tu2	1.3	0.0026	0.13	0.0025	0.0041	0.0092	0.076	0.000020	0.17	0.00059	0.0012
Tu3	1.4	0.0027	0.12	0.0022	0.0037	0.0087	0.088	0.000028	0.16	0.00065	0.0014
Tu4	1.8	0.0033	0.15	0.0029	0.0040	0.0093	0.090	0.000026	0.20	0.00079	0.0016
Tu5	1.5	0.0029	0.14	0.0027	0.0049	0.0098	0.870	0.000026	0.20	0.00068	0.0015
Tu6	1.7	0.0035	0.18	0.0039	0.0045	0.0085	0.055	0.000056	0.19	0.00056	0.0015
Tu7	1.9	0.0026	0.15	0.0042	0.0078	0.0025	0.066	0.000078	0.29	0.00066	0.0013
Tu8	2.1	0.0011	0.17	0.0036	0.0028	0.0048	0.021	n.r.	0.16	0.00011	0.0018
Tu9	2.1	0.0018	0.18	0.0023	0.0015	0.0041	0.074	0.000059	0.12	0.00017	0.0021
Tu10	2.5	0.0041	0.12	0.0027	0.0039	0.0027	0.052	0.000047	0.21	0.00031	0.0026
Tu11	1.9	0.0024	0.14	0.0024	0.0047	0.0028	0.056	0.000066	0.17	0.00025	0.0015
Tu12	1.7	0.0031	0.19	0.0042	0.0056	0.0036	0.047	0.000079	0.18	0.00029	0.0008
Tu13	1.8	0.0028	0.12	0.0032	0.0042	0.0029	0.053	0.000038	0.16	0.00017	0.0011

b.d.l. below detection limit

Hydrogen and CO rapidly respond to changes of temperature–redox conditions (Giggenbach 1987), thus their concentrations tend to readjust during the uprising of hydrothermal–magmatic gases toward the surface, according to the following pressure-independent reaction:

$$CO_2 + H_2 \leftrightarrow CO + H_2O \quad (1)$$

The temperature dependence of the equilibrium constant of reaction (1) is given by Giggenbach (1996):

$$\log(X_{CO}/X_{CO2}) - \log(X_{H2}/X_{H2O}) = 2.49 - 2248/T \quad (2)$$

where T is in K and X_{CO}, X_{CO2}, X_{H2}, and X_{H2O} are the molar fractions of CO, CO_2, H_2, and H_2O, respectively. As shown in Fig. 2, CO and H_2 seem to attain equilibrium in a single vapor phase at temperatures between 160 and 200 °C and R_H values ranging from −3 to −3.5. The relatively low H_2 and CO concentrations of the Tu12 sample, which plots far from the other Tupungatito gases, are likely related to the extremely low flux of this fumarole, which favors oxidation of these highly reactive gas compounds at shallow depth. The R_H values controlling the equilibrium of reaction (1) are slightly more negative than that inferred by the FeO–$FeO_{1.5}$ "rock"

Table 3 Isotopic composition of steam ($\delta^{18}O$ and δD in per mille vs. V-SMOW), carbon in CO_2 ($\delta^{13}C$ in per mille vs. V-PDB), helium (as R/Ra, where R is the measured ratio and Ra is that of the air: 1.39×10^{-6}; Mamyrin and Tolstikhin 1984), and argon ($^{40}Ar/^{36}Ar$) for the Tupungatito thermal discharges. $\delta^{18}O$ and δD values of local precipitations (MW), as well as ^{36}Ar and radiogenic Ar ($^{40}Ar^*$) concentrations and He/Ne, $^{40}Ar^*/^4He$, $CO_2/^3He$, and $CH_4/^3He$ ratios, are also reported

	R/Ra	$^{40}Ar/^{36}Ar$	^{36}Ar	$^{40}Ar^*$	$^{40}Ar^*/^4He$	He/Ne	$\delta^{13}C\text{-}CO_2$	δD	$\delta^{18}O$	$CO_2/^3He$	$CH_4/^3He$
Tu1	5.45	327	0.000012	0.00039	0.470	56	−7.65	−68	−2.9	1.54E+11	6.99E+07
Tu2							−6.92	−72	−3.3		
Tu3	5.19	374	0.000015	0.0012	1.281	38	−8.16	−55	0.8	1.43E+11	4.32E+07
Tu4							−6.84	−50	−0.6		
Tu5	5.26	415	0.000009	0.00113	1.490	551	−7.11	−67	−2.2	1.75E+11	5.90E+07
Tu6	5.23	366	0.000010	0.00073	1.284	105	−6.12	−65	−1.8	2.37E+11	5.50E+07
Tu7	6.09	352	0.000013	0.00072	0.881	326	−6.74	−53	−1.1	1.41E+11	4.42E+07
Tu8	5.06	304	0.000104	0.00088	0.803	37	−0.30			1.27E+11	2.79E+07
Tu9	5.16	415	0.000015	0.00176	3.137	212	−5.31	−75	−3.3	2.44E+11	4.66E+07
Tu10	5.41	461	0.000014	0.00237	3.590	336	−6.29	−50	−0.5	1.95E+11	7.27E+07
Tu11							−6.56	−70	−3.1		
Tu12	5.78	388	0.000015	0.00138	2.426	195	−6.67	−54	−0.8	2.14E+11	9.06E+07
Tu13							−7.31				

n.a. not analyzed

Table 4 Temperature (in degree Celsius), pH and chemical composition (in milligram per liter) of the Tupungatito crater lake (CL)

	Date	Coord. N	Coord E	Altitude	T	pH	F^-	Cl^-	SO_4^{2-}	Br^-	Na^+	NH_4^+	K^+	Mg^{2+}	Ca^{2+}
CL	2/16/2011	6305292	423220	5204	32.2	0.34	210	12500	12600	21	590	240	360	310	1100

buffer (−2.8). This difference is presumably caused by the presence of SO_2 (Table 1), which is reduced to H_2S at lower R_H values (Giggenbach 1987). However, steam condensation, which has likely affected these low temperature gas discharges, may also control the H_2/H_2O ratios, as H_2 can be partitioned between water and saturated vapor water according to its distribution coefficient (B_{H2}), which ranges from 4.84 (at 100 °C) to 0 at the critical point. In this way, to produce an R_H decrease of 0.2–0.7 (i.e., the difference between −2.8 and the measured R_H values) at the H_2–CO equilibrium temperatures (from 160 to 200 °C), the fraction (c) of separated condensed steam (a parameter that ranges from 0 to 1) would have to be in the range from 0.05 to 0.20.

Application of equilibrium thermodynamics in the H_2–CO_2–CO–CH_4–H_2O system can provide useful insights for evaluating temperature and redox conditions that control hydrothermal-magmatic fluids (Chiodini and Marini 1998). This approach is based on reaction (1) and other four reactions, as follows:

$$3CO_2 + CH_4 \leftrightarrow 4CO + 2H_2O \quad (3)$$

$$CH_4 + 2H_2O \leftrightarrow 4H_2 + CO_2 \quad (4)$$

$$CH_4 + H_2O \leftrightarrow 3H_2 + CO \quad (5)$$

$$CH_4 + CO_2 \leftrightarrow 2H_2 + 2CO \quad (6)$$

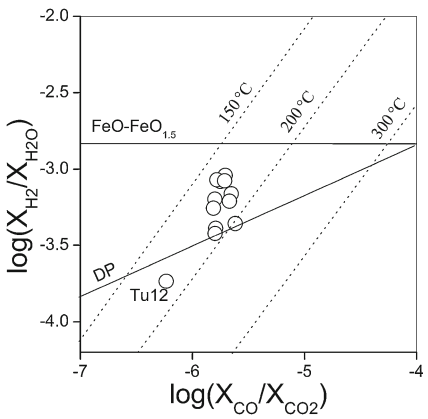

Fig. 2 $Log(X_{CO}/X_{CO2})$ vs. $log(X_{H2}/X_{H2O})$ binary diagram. *Solid curves* refer to the DP (D'Amore and Panichi 1980) and $FeO–FeO_{1.5}$ (Giggenbach 1987) redox buffers

The equations describing the dependence on temperature of reactions (1), (3), (4), (5), and (6) can be combined in the redox independent $[\log(X_{CO}/X_{CO2})+\log(X_{H2O}/X_{H2})]$ and $[3\log(X_{CO}/X_{CO2})+\log(X_{CO}/X_{CH4})]$ functions. In the $[\log(X_{CO}/X_{CO2})+\log(X_{H2O}/X_{H2})]$ vs. $[3\log(X_{CO}/X_{CO2})+\log(X_{CO}/X_{CH4})]$ binary diagram (Fig. 3), the theoretical compositions of (1) single saturated vapor phase (vapor); (2) single saturated liquid phase (liquid); (3) vapors produced by single-step vapor separationfrom boiling liquids of original temperature T_o=150, 200, 250, 300, and 350 °C (dashed lines); and (4) single saturated vapor phase after separation at T=100 °C of different fractions (c) of condensed steam (dotted lines), are reported (Chiodini and Marini 1998). According to this approach, the Tupungatito fumaroles, with the exception of the Tu12 sample, seem to equilibrate in a single vapor phase at ~220 °C. These calculated temperatures are significantly higher than those calculated on the basis of Eq. (2), since reactions (3)–(6), which include CH_4, have a slower kinetics with respect to that of reaction (1) (Giggenbach 1997; Taran and Giggenbach 2003). Although the fractions (c) of condensed steam, ranging from 0.1 to 0.6, are higher than those evaluated on the basis of water–vapor distribution coefficient of H_2 values (i.e., possibly due to uncertainties in the assumptions of the two approaches), both results show that steam condensation is a significant process affecting the hydrothermal–magmatic fluids feeding the Tupungatito fumaroles.

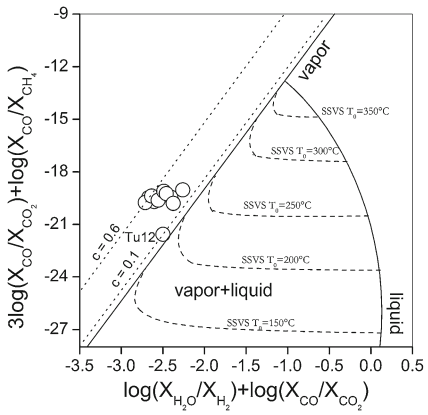

Fig. 3 $3\log(X_{CO}/X_{CO2})+\log(X_{CO}/X_{CH4})$ vs. $\log(X_{CO}/X_{CO2})-\log(X_{H2}/X_{H2O})$ binary diagram. The theoretical values for a single saturated vapor phase (vapor) and single saturated liquid phase (liquid) are shown. Compositions of (1) vapors separated in a single step from boiling liquids at T_o=150, 200, 250, 300, and 350 °C (*dashed lines*) and (2) single vapor phase affected by separation at T=100 °C of different fractions (c=0.3 and c=0.7) of condensed steam (dotted lines), are also reported

Dehydrogenation processes involving the C_2 and C_3 alkene–alkane pairs may also be used to obtain insights on chemical–physical conditions of the deep fluid source regions (Capaccioni and Mangani 2001; Seewald 2001; Taran and Giggenbach 2003; Tassi et al. 2005b). Dehydrogenation of C_2H_6 and C_3H_8 to produce C_2H_4 and C_3H_6, respectively, are given by:

$$C_2H_6 \leftrightarrow C_2H_4 + H_2 \quad (7)$$

$$C_3H_8 \leftrightarrow C_3H_6 + H_2 \quad (8)$$

Using thermochemical data reported by Reid et al. (1987), Barin (1989), and Domalski and Hearing (1993), in the equilibrated vapor the temperature dependence of equilibrium constant for reactions (7) and (8) are (Capaccioni et al. 2004):

$$\log(P_{C2H4}/P_{C2H6}) = 7.43 - 7809/T - \log P_{H2} \quad (9)$$

$$\log(P_{C3H6}/P_{C3H8}) = 7.15 - 6000/T - \log P_{H2} \quad (10)$$

where T is in K and $P_{H2}=P_{tot}\times X_{H2}$. Considering that changes of $\log P_{H2O}$ ($P_{tot}\sim P_{H2O}$) with temperature for coexisting vapor and liquid water are described by $\log P_{H2O}=5.51-2048/T$; Giggenbach 1980), Eqs. (9) and (10) can be expressed, as follows:

$$\log(P_{C2H4}/P_{C2H6}) = 1.92 - 5761/T - R_H \quad (11)$$

$$\log(P_{C3H6}/P_{C3H8}) = 1.64 - 4552/T - R_H \quad (12)$$

At the equilibrium temperatures calculated on the basis of the H_2–CO_2–CO–CH_4–H_2O system (~220 °C), the C_2H_4–C_2H_6 equilibrium is attained at R_H values ranging from −6.5 to −7.1consistentwith those of the SO_2–H_2S redox buffer for SO_2/H_2S ratio of 10, i.e., 3 orders of magnitude higher than the measured SO_2/H_2S ratio (0.005–0.02; Fig. 4). The C_3H_6–C_3H_8 pair equilibrates at more reducing conditions (R_H=−5.7÷−6) than those of the C_2H_4–C_2H_6 pair (Fig. 5, possibly because the C_3–C_3 pair attained equilibrium at shallower depth, i.e., where the influence of magmatic gases is less, than the C_2–C_2 pair, reaction (9) being characterized by a slower kinetics with respect to reaction (10) (Lide 2001; Seewald 2001; Capaccioni et al. 2004).

Fumarolic fluid sources

The relatively low outlet temperatures of the Tupungatito fumaroles (from 80.8 to 83.6 °C), which are close to the boiling point of water at 5,200 m a.s.l. (~82.3 °C), unequivocally indicate that liquid water occurs at shallow depth, likely as a result of steam condensation affecting the uprising fluids (Stevenson 1993), although a mixture of both hot magmatic gases and groundwater, forming a boiling solution, which at its turn separates at shallow depth, cannot be excluded (Taran et al. 1997). The δD–H_2O vs. $\delta^{18}O$–H_2O binary diagram (Fig. 6a), where the Global Meteoric Water Line (GMWL; Craig 1961) is reported, shows that the origin of water vapor of the Tupungatito fumaroles, as well as those from Alitar, Irrupucuntu, Lascar, Lastarria, Olca, Putana, and Tacora volcanoes (Tassi et al. 2009a, b, 2011; Aguilera et al. 2012; Capaccioni et al. 2011), are related to mixing processes between meteoric (MW) and "andesitic" (Taran et al. 1989; Giggenbach 1992a) water. If we assume that steam is produced by a simple mixing between these two end members, the position of the Tupungatito samples in Fig. 6a apparently corresponds to 52–69 % of magmatic water.

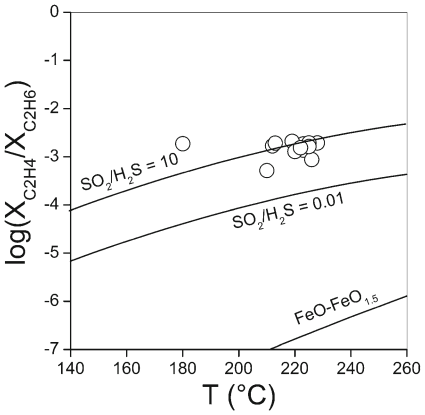

Fig. 4 Binary diagram of $\log(X_{C2H4}/X_{C2H6})$ vs. calculated temperatures (in degree Celsius) in the H_2–CO_2–CO–CH_4–H_2O system. *Solid curves* refer to SO_2–H_2S (SO_2/H_2S equal to 10 and 0.01) and FeO–$FeO_{1.5}$ redox buffer (Giggenbach 1996)

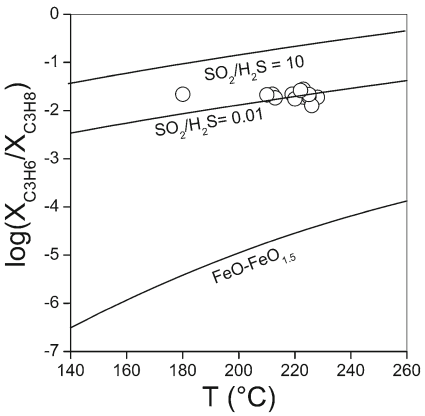

Fig. 5 Binary diagram of $\log(X_{C3H6}/X_{C3H8})$ vs. calculated temperatures (degree Celsius) in the H_2–CO_2–CO–CH_4–H_2O system. Solid curves refer to SO_2–H_2S (SO_2/H_2S equal to 10 and 0.01) and FeO–$FeO_{1.5}$ redox buffer (Giggenbach 1996)

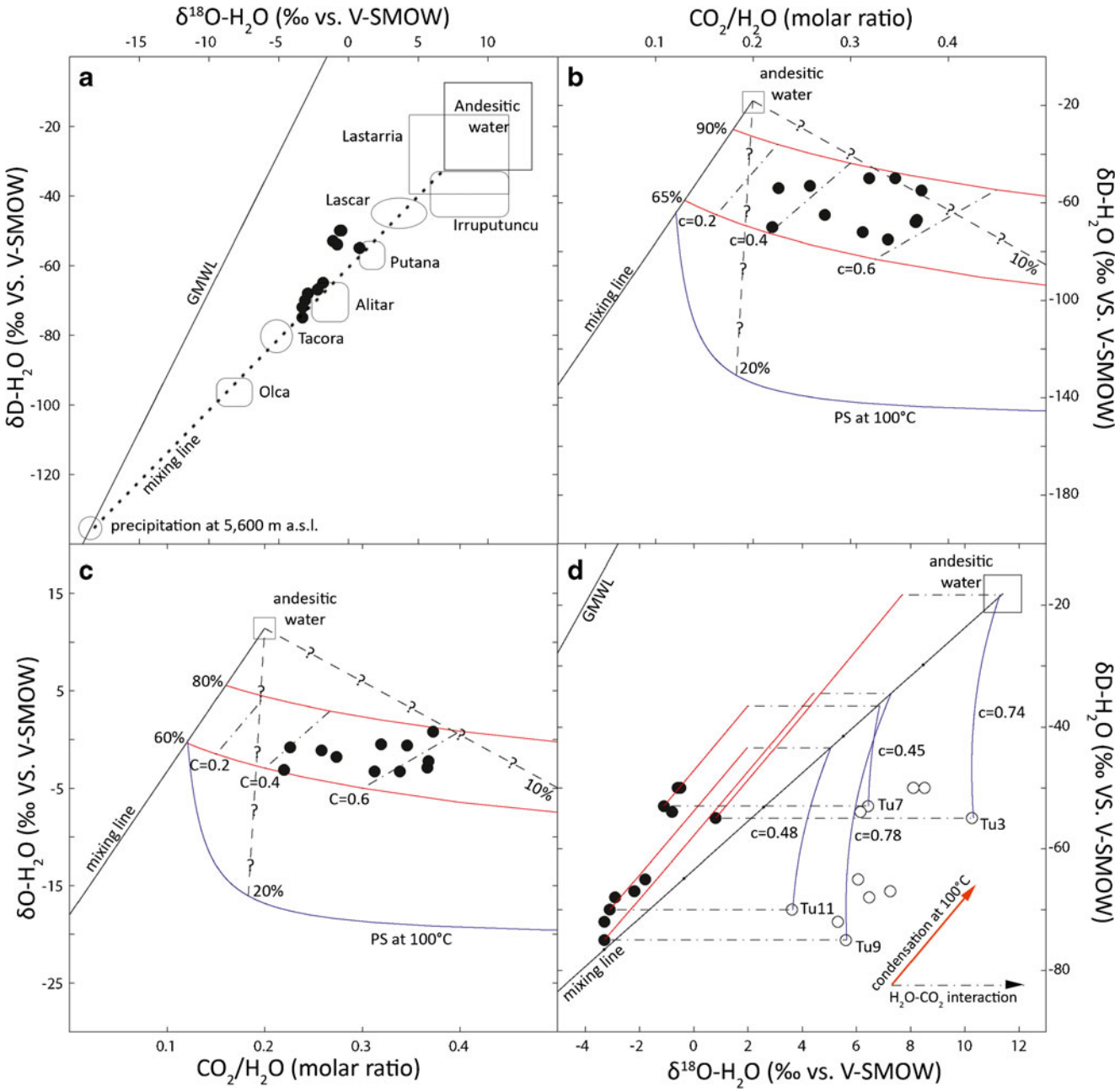

Fig. 6 **a** $\delta^{18}O$–H_2O vs. δD–H_2O diagram of steam from the Tupungatito fumaroles. Andesitic water field (Taran et al. 1989; Giggenbach 1992a, b), Global Meteoric Water Line (GMWL; Craig 1961), isotopic composition of the meteoric water (MW) at 5,600 m a.s.l. ($\delta D \sim -135‰$ and $\delta^{18}O \sim -18‰$; Capaccioni et al. 2011), mixing line between meteoric and Andesitic water, and isotopic composition of Alitar, Irrupucuntu, Lascar, Lastarria, Olca, Putana, and Tacora volcanoes (Tassi et al. 2005a, b, 2011; Aguilera et al. 2012; Capaccioni et al. 2011) are reported. **b**–**c** CO_2/H_2O molar ratio vs. δD–H_2O and CO_2/H_2O molar ratio vs. $\delta^{18}O$–H_2O diagrams of steam from the Tupungatito fumaroles. Andesitic water field (Aguilera et al. 2012), mixing line between meteoric and Andesitic water, condensation curves which represent initial mixture of 65 and 90 % magmatic vapor, condensed steam fraction ranging from 0.2 to 0.6, "Primary Steam" line at 100 °C (Taran et al. 1997), and mixing lines between Andesitic water and 10 and 20 % of "Primary Steam" are reported. **d** Detail of the $\delta^{18}O$–H_2O vs. δD–H_2O diagram of steam from the Tupungatito fumaroles. Isotopic compositions produced by(1) steam condensation at 100 °C (*solid red line*) and (2) H_2O–CO_2 isotopic exchange from 220 °C to outlet temperatures, calculated for condensed steam fraction (*c*) ranging from 0 to 0.78, were also reported (*solid blue line*)

However, if steam condensation occurs, both the chemical composition (e.g., CO_2/H_2O ratio) and the isotopic signature of water vapor in the fumarolic discharges are expected to be affected (e.g., Taran et al. 1997; Chiodini et al. 2001; Ohba 2007; Ohba et al. 2011a, b; Shinohara et al. 2011). The composition of the gas phase after the partial condensation

of the water vapor can be modeled by the Rayleigh fractionation process, expressed by:

$$\delta = (\delta_i + 1{,}000)F^{\alpha-1} - 1{,}000 \quad (13)$$

$$r = r_i F^{(1/\beta-1)} \quad (14)$$

where δ indicates the delta notation of D/H and $^{18}O/^{16}O$ of H_2O; F is the fraction of H_2O vapor left after condensation; α is the isotope fractionation factor between liquid water and vapor for O and H isotopes (1.00509 and 1.0283 at 100 °C, respectively; Horita and Cole 1994); r is the CO_2/H_2O molar ratio; β corresponds to the CO_2/H_2O distribution factor between liquid water and vapor (0.000215 at 100 °C; Giggenbach 1980); and the subscript i is the initial value of the gas before condensation.

Assuming a CO_2/H_2O ratio for meteoric water equal to zero (Taran et al. 1997) and considering the fumarolic gases from Lastarria as the most representative end-member of "Andesitic water" for the Andean volcanoes due to its physical–chemical characteristics (e.g., T up to 400 °C, CO_2/H_2O up to 0.2, δD up to −18.1, $\delta^{18}O$ up to 10.7l Aguilera et al. 2012), Fig. 6b, c show the change in the CO_2/H_2O ratio and δD–$\delta^{18}O$ of H_2O due to condensation. According to this approach, the Tupungatito fumaroles are distributed between the condensation curves that represent initial mixtures between 60 and 90 % of magmatic vapor with condensed steam fraction values (c=1−F) ranging from 0.2 to 0.6 (F ranging between 0.4 and 0.8), similar to those obtained in Fig 3. Figure 6b, c also show the "Primary steam" (PS) line, which represents the composition of steam generated at shallow depth (100 °C) by mixing of meteoric water and magmatic vapor (at 10 and 900 °C, respectively; Taran et al. 1997). The Tupungatito fumaroles could also be explained as a mixture between Andesitic water and 10–20 % of PS. However, this cannot simply be evaluated with a mixing line, because a mixture between >50 % magmatic fluids and "Primary Steam", as calculated for the Tupungatito samples (Fig. 6b, c), will not produce a fumarolic gas at boiling temperatures (~82 °C). Thus, the hypothesis of a mixing between magmatic fluids and vapor derived from a shallow evaporated aquifer can likely be discarded. The higher condensed steam fraction values and lower initial mixtures calculated in the CO_2/H_2O–$\delta^{18}O$–H_2O plot (Fig. 6c) with respect to Fig. 6b can be attributed to ^{18}O re-equilibration between H_2O and CO_2 (Fig. 6d), which shifts the initial $\delta^{18}O$ data to lower values. Following the approach proposed by Chiodini et al. (2000), isotopic fractionation related to H_2O–CO_2 interactions were calculated according to the following equation:

$$\delta^{18}O\text{–}H_2O_{ini} = \delta^{18}O\text{–}H_2O + [2X_{CO2}/(1 + X_{CO2})] \times [1000\ln\alpha(T_i) - 1000\ln\alpha(T_{meas})] \quad (15)$$

where T_i is 220 °C (which is the average of the H_2–CO_2–CO–CH_4–H_2O equilibrium temperatures excluding the Tu12 sample; Fig. 3), $\delta^{18}O$–H_2O_{ini} represents the $\delta^{18}O$–H_2O composition of steam at the H_2–CO_2–CO–CH_4–H_2O equilibrium conditions, T_{meas} is the fumarolic outlet temperature, X_{CO2} is the CO_2 molar fraction, and α is the oxygen isotope fractionation factor between $CO_{2(g)}$ and $H_2O_{(g)}$, whose temperature dependence can be described, as follows (Chiodini et al. 2000):

$$1{,}000\ln\alpha = -5.7232 + 20.303(10^3/T) - 11.977(10^6/T^2) + 3.7432(10^9/T^3) \quad (16)$$

Equation (15) shows that the initial $\delta^{18}O$–H_2O value depends on both $\delta^{18}O$–H_2O and X_{CO2} values, which at their turn depend on the fraction of H_2O vapor left after condensation (F). Using Eq. (13), the initial values of the gas before condensation were calculated and plotted in Fig. 6d (solid red lines). The fractionation lines (dotted black lines) on Fig. 6d were constructed by applying Eq. (15), using the $\delta^{18}O$–H_2O and X_{CO2} values calculated for the effects of steam condensation by Eqs. (13) and (14) (blue solid lines). The X_{CO2} values were calculated considering that water vapor and CO_2 are the most common gases in volcanic systems (X_{CO2}+X_{H2O}~1; Giggenbach 1980). The interceptions between solid blue lines and the MW–andesitic water mixing line (solid black line; Fig. 6d) indicate that (1) the fraction of magmatic water in vapors equilibrated in the H_2–CO_2–CO–CH_4–H_2O system ranges from 78 to 99 % (samples Tu11 and Tu3, respectively) and (2) c ranges from 0.45 to 0.78 (samples Tu7 and Tu9, respectively), consistent with the condensate fraction values estimated above (Figs. 3 and 6b, c).

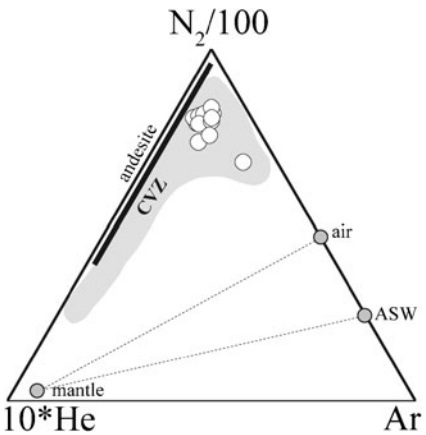

Fig. 7 N_2/100-Ar-He*10 diagram for the Tupungatito thermal discharges (Giggenbach 1992b). Air and Air Saturated Waters (ASW) compositions and convergent plate boundaries ("andesite") field (Giggenbach 1996) are also reported. The compositional fields (SVZ) of the Lastarria, Lascar, Irrupucuntu, Putana, Alitar, Olca, and Tacora fumarolic gases (Tassi et al. 2009a, 2011; Aguilera et al. 2012; Capaccioni et al. 2011) are plotted for comparison

The dominant magmatic signature of the vapor isotopes is consistent with the occurrence of SO_2, HCl, and HF in the fumarolic fluids (Table 1). Hence, the liquid dominated system, whose boiling produces vapors feeding the Tupungatito fumaroles, is not able to completely scrub the highly soluble and reactive gases released from the magmatic source, possibly because it is not well developed and has a low pH (Symonds et al. 2001). The $CH_4/(C_2H_6+C_3H_8)$ ratios (from 83 to 223) of the fumarolic fluids are significantly higher than those typically measured in hydrothermal fluids (<100) from sedimentary and volcanic domains (e.g., Oremland et al. 1987; Whiticar and Suess 1990; Jenden et al. 1993; Whiticar 1999; Zelenski and Taran 2011; Tassi et al. 2012). The CH_4 excess may be caused by the relatively low stability of C_{2+} compounds with respect to that of CH_4 under relatively high temperatures. The occurrence of comparable amounts of (1) alkenes (C_2H_4, C_3H_6, and C_4H_8) and furan (C_4H_4O), formed at oxidizing conditions and relatively high temperatures (Capaccioni et al. 1995), and (2) aromatics (C_6H_6 and C_7H_8) and thiophene (C_4H_4S), produced by catalytic reactions favored at reducing conditions (Tassi et al. 2010), corroborate the hypothesis that the Tupungatito gas discharges are mostly sourced by magmatic fluids interacting with a limited hydrothermal aquifer, which is not able to reduce all the gas species formed at oxidizing conditions.

The ternary N_2–Ar–He diagram (Fig. 7) proposed by Giggenbach (1992b) is commonly used to constrain potential sources of these gases, such as crustal and mantle fluids, and air contamination. The Tupungatito fumaroles show very high N_2/Ar ratios (up to 1,479) relative to air (83.6), typical of arc volcanoes including those of CVZ (Tassi et al. 2009a, 2011; Aguilera et al. 2012; Capaccioni et al. 2011). This indicates a non atmospheric source for N_2, suggesting that (1) the mantle source is affected by contamination of organic-rich sediments in the subducted slab (Matsuo et al. 1978; Jenden et al. 1988; Giggenbach 1997; Snyder et al. 2003) and (2) possible addition of crustal fluids to the magmatic system. This hypothesis is also supported by the helium isotopic composition (R/Ra from 5.06 to 6.09), which is consistent with the wide R/Ra range characterizing fluids related to continental and arc volcanoes (between 3 and 8; Craig and Lupton 1976; Poreda and Craig 1989; Ballentine and Sherwood Lollar 2002; Hilton et al. 2002).

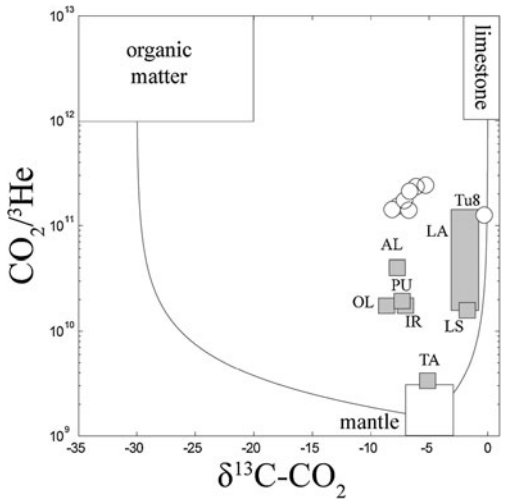

Fig. 8 $CO_2/^3He$ vs. $\delta^{13}C$–CO_2 diagram for the Tupungatito gas discharges. Gases from organic-rich sediments (S), limestone (L) and mantle (M) (Sano and Marty 1995) are reported. The compositional fields of the Lastarria (*LS*), Lascar (*LA*), Irrupucuntu (*IR*), Putana (*PU*), Alitar (*AL*), Olca (*OL*), and Tacora (*TA*) volcanoes (Tassi et al. 2009a, 2011; Aguilera et al. 2012; Capaccioni et al. 2011) gases are plotted for comparison

The $CH_4/^3He$ ratios ($2.79–9.06\times10^7$; Table 3) are significantly higher than those measured in sediment-free mid-ocean ridge environment (between 1×10^5 and 1×10^6; Snyder et al. 2003), suggesting significant contribution of crustal fluids rich in both thermogenic and/or biogenic CH_4, which is consistent with the "crustal signatures" of the Tupungatito lavas ("Geodynamic, geological, and volcanological settings" section). Unfortunately, isotope data of CH_4, which are useful to discriminate different mechanisms for the origin of this compound (e.g., Schoell 1980, 1988), are not available for the Tupungatito gases.

The $^{40}Ar/^{36}Ar$ ratios (from 304 to 461) are higher than that of air (295.5), indicating that 3–36 % of the Ar is likely related to the radiogenic decay of ^{40}K, the latter being typically enriched in the crust. Fluids from the upper mantle can also be considered an important source of ^{40}Ar-enriched fluids, although ^{40}Ar concentrations are not homogeneously distributed in the mantle since MORB lavas are characterized by $^{40}Ar/^{36}Ar$ ratios up to 28,000 (Sarda et al. 1985; Farley and Poreda 1993). By assuming that ^{36}Ar is entirely derived from air and $^{40}Ar/^{36}Ar$ ratio in air=295.5, the concentration of radiogenic Ar ($^{40}Ar^*$) in gas samples can be calculated, as follows:

$$^{40}Ar* = {}^{40}Ar - 295.5\times{}^{36}Ar \quad (17)$$

The $^{40}Ar^*/^4He$ ratio is a useful tracer of noble gas fractionation during volatile exsolution from magma (Marty 1995; Sarda and Moreira 2002). The $^{40}Ar^*/^4He$ ratio produced by the present-day radiogenic decaying process in the mantle, calculated on the basis of measured $K/(U+Th)$ ratios in MORB and the "bulk earth" value of 0.55 for 4.5 Ga of radiogenic production is ~0.27±0.02 (Jochum et al. 1983), a value slightly lower than those of Tupungatito gases (from 0.47 to 3.59; Table 3).

The $CO_2/^3He$ ratios and the $\delta^{13}C$–CO_2 values are commonly used as diagnostic parameters to distinguish fluid contributions from crust, mantle and atmosphere (Marty and Jambon 1987; O'Nions and Oxburg 1988). The $CO_2/^3He$ ratios in the Tupungatito fumaroles range from 1.27×10^{11} to 2.44×10^{11} (Table 3), i.e., more than 1 order

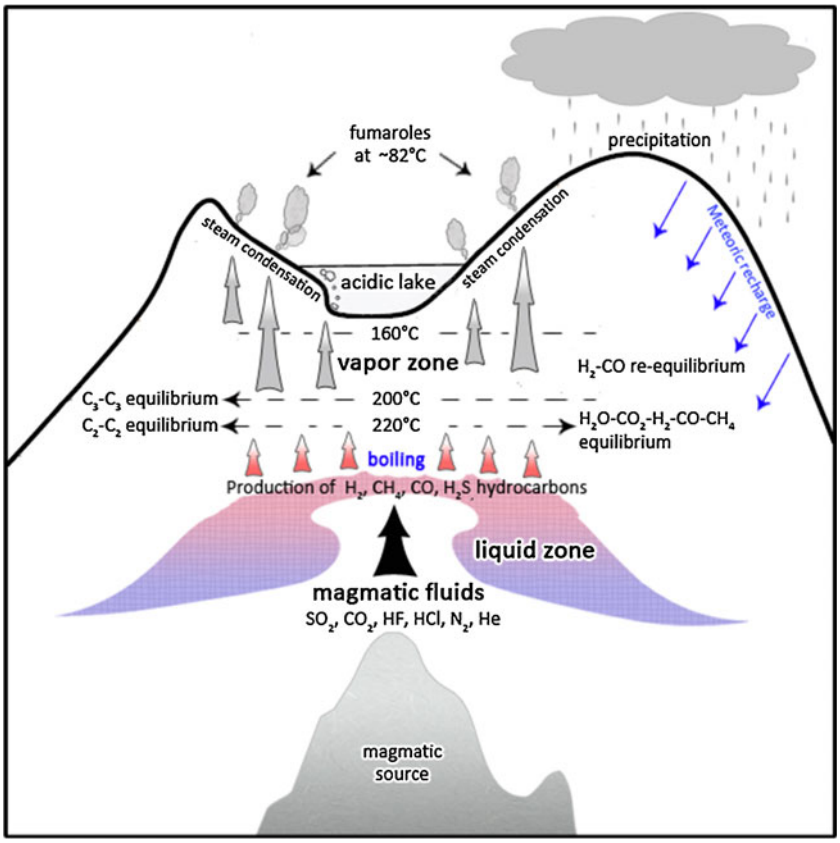

Fig. 9 Conceptual geochemical model of fluid circulation at the Tupungatito volcanic system

of magnitude higher than the MORB ratio (1.41×10^9; Marty and Jambon 1987; Sano and Marty 1995). This suggests that CO_2 is not only related to mantle (M) degassing, but it partially derives from limestone (L) and/or organic-rich sediments (S). The relative contribution of each one of these potential CO_2 sources can be evaluated, as follows (Sano and Marty 1995):

$$M + S + L = 1 \tag{18}$$

$$\begin{aligned}\left(\delta^{13}C{-}CO_2\right)_{\text{meas}} &= M\left(\delta^{13}C{-}CO_2\right)_{\text{MORB}} \\ &+ L\left(\delta^{13}C{-}CO_2\right)_{\text{Lim}} \\ &+ S\left(\delta^{13}C{-}CO_2\right)_{\text{Sed}}\end{aligned} \tag{19}$$

$$\begin{aligned}\left[1/\left(CO_2/^3He\right)\right]_{\text{meas}} &= \left[M/\left(CO_2/^3He\right)\right]_{\text{MORB}} \\ &+ \left[L/\left(CO_2/^3He\right)\right]_{\text{Lim}} \\ &+ \left[S/\left(CO_2/^3He\right)\right]_{\text{Sed}}\end{aligned} \tag{20}$$

where subscripts meas, MORB, Lim, and Sed refer to the sample, MORB (a proxy to the upper mantle), limestone, and organic sediment, respectively.

Following Sano and Marty (1995), we assume that the end members have the following values:

$$\begin{aligned}\left(\delta^{13}C{-}CO_2\right)_{\text{MORB}} &= -5‰;\ \left(\delta^{13}C{-}CO_2\right)_{\text{Sed}} \\ &= -30‰;\ \left(\delta^{13}C{-}CO_2\right)_{\text{Lim}} = 0‰;\ \left(CO_2/^3He\right)_{\text{MORB}} \\ &= 1.5\times10^9;\ \left(CO_2/^3He\right)_{\text{Sed}} \\ &= 1\times10^{13};\ \left(CO_2/^3He\right)_{\text{Lim}} = 1\times10^{13}\end{aligned}$$

According to Eqs. (18), (19), and (20), CO_2 is mostly produced from carbonates of the subducting slab and the basement (L >70 %), whereas sediments are to be regarded as a secondary CO_2 source. These results are consistent with those of fluid discharges from several volcanoes of the CVZ, such as Alitar, Olca, Putana, and Irrupucuntu (Tassi et al. 2011), whereas gases from Tacora, Lascar, and Lastarria volcanoes (Tassi et al. 2009a; 2011; Aguilera et al. 2012; Capaccioni et al. 2011), which are located in the same area, plot between M and L CO_2 sources with S <10 % (Fig. 8). This implies that subducted slab age (Eocene at 17.5°S to Quaternary at 46°S; Ramos et al. 2004), slab thermal state (Grevemeyer et al. 2003), and type and amount of material subducted (von Huene and Scholl 1991; Strand 1995; Contreras-Reyes et al. 2010), which significantly change from north to south along the Chilean margin, do not have

a significant influence on the $CO_2/^3He$ and $\delta^{13}C–CO_2$ ratios. In contrast, the relative proportions of hydrothermal and magmatic gases, a feature peculiar to each volcano that depends on its state of activity and fluid circulation pattern, seem to exert a strong control on chemical and isotopic compositions of He and CO_2. Separation of solid (such as calcite) and liquid phases likely occurring during fluid uprising may explain the measured variations of the $\delta^{13}C–CO_2$ values in the Tupungatito fumaroles (from −8.16 to −5.31‰ vs. V-PDB; Table 3; e.g., Ray et al. 2009; de Leeuw et al. 2010). The high $\delta^{13}C$-CO_2 value (−0.30‰ vs. V-PDB; Table 3) of the bubbling gas sample (Tu8) might be due to kinetic fractionation processes related to the lake degassing temperature (>30 °C) and relative proportions of the different carbon species (e.g., Mook et al. 1974) dissolved in the lake and not to a different carbon source.

Conclusions

The fumarolic activity at Tupungatito volcano is related to uprising of magmatic fluids partially scrubbed by a hydrothermal aquifer, whose boiling produces vapors that are affected by steam condensation as they approach the surface. The $\delta^{13}C–CO_2$ and $CO_2/^3He$ ratios suggest (1) mantle contamination by limestone from the subducting Nazca Plate and/or (2) interaction between the magmatic source and the crustal basement. However, the helium isotopic composition (R/Ra from 5.06 to 6.09), $CH_4/^3He$ ratios ($2.8–9.1\times10^6$) as well as the "crustal signatures" of the Tupungatito lavas, suggest that the contribution of crustal fluids is likely an important process controlling the composition of the Tupungatito fluids.

A conceptual geochemical model of the Tupungatito fluid circulation pattern, showing fluid source regions and chemical physical conditions inferred by chemical equilibrium regulating the composition of gases at different depths, is plotted in Fig. 9. Primary fluids originating from magma degassing are partially "filtered" by an overlying aquifer whose boiling produces gases enriched in reduced gas species, such as H_2, CO, CH_4, and H_2S. Fumarolic fluids show the signature of a magmatic source (CO_2, He, N_2, SO_2 HCl, HF, and andesitic water), notwithstanding the fact that they are affected by condensation of a significant (up to 0.78) steam fraction. Chemical reactions in the $H_2O–CO_2–CH_4–CO–H_2$ system attain equilibrium in a separated vapor phase at a temperature ~220 °C, where the C_2 alkane–alkene pair also equilibrates under redox conditions typical of an environment dominated by magmatic fluids. On the contrary, dehydrogenation of C_3H_8 re-equilibrates at more reducing conditions and/or lower temperatures. Chemical reactions regulating H_2 and CO, rapidly responding to changes of chemical–physical conditions affecting the uprising hydrothermal–magmatic vapors, record temperatures down to 160 °C and redox conditions approaching those of the hydrothermal "rock" buffer.

The results presented in this work can be used for future geochemical monitoring programs due to the recent and relatively intense volcanic activity showed by Tupungatito volcano in the last 180 years.

Acknowledgments This research was partly funded by the PBCT-PDA07 project granted by CONICYT (Chilean National Commission for Science and Technology). Additional support was provided by MECESUP doctoral fellowship (UCH-0708) and by FONDAP Proyect #15090013 "Centro de Excelencia en Geotermia de los Andes, CEGA". The authors acknowledge the additional support provided by the University of Florence (Laboratory of Fluid and Rock Geochemistry, Department of Earth Sciences and CNR-IGG). Careful and thoughtful suggestions of Y. Taran and J. Varekamp were warmly appreciated.

References

Aguilera F, Tassi F, Darrah T, Moune S, Vaselli O (2012) Geochemical model of a magmatic hydrothermal system at the Lastarria Volcano, Northern Chile. Bull Volcanol 74:119–134

Ballentine CJ, Sherwood Lollar B (2002) Regional groundwater focusing of nitrogen and noble gases into the Hugoton-panhandle giant gas field, USA. Geochim Cosmoch Acta 66–14:2483–2497

Barazangi M, Isacks B (1976) Spatial distribution of earthquakes and subduction of the Nazca plate beneath South America. Geology 4:606–692

Barin I (1989) Thermochemical data on pure substances, vol 1. Wenheim, Germany

Brantley SL, Agustsdottir AM, Rowe GL (1993) Crater lakes reveal volcanic heat and volatile fluxes. Geol Soc Am Today 3:175–178

Cande S, Leslie R (1986) Late Cenozoic tectonics of the southern Chile Trench. J Geophys Res 91:471–496

Cande S, Leslie R (1987) Interaction between the Chile Ridge and Chile Trench: geophysical and geothermal evidence. J Geophys Res 92:495–520

Capaccioni B, Martini M, Mangani F (1995) Light hydrocarbons in hydrothermal and magmatic fumaroles: hints of catalytic and thermal reactions. Bull Volcanol 56:593–600

Capaccioni B, Mangani F (2001) Monitoring of active but quiescent volcanoes using light hydrocarbon distribution in volcanic gases: the results of 4 years of discontinuous monitoring in the Campi Flegrei (Italy). Earth Planet Sci Lett 188:543–555

Capaccioni B, Taran Y, Tassi F, Vaselli O, Mangani G, Macias JL (2004) Source conditions and degradation processes of light hydrocarbons in volcanic gases: an example from El Chichón volcano (Chiapas State, Mexico). Chem Geol 206:81–96

Capaccioni B, Aguilera F, Tassi F, Darrah T, Poreda RJ, Vaselli O (2011) Geochemical and isotopic evidences of magmatic inputs in the hydrothermal reservoir feeding the fumarolic discharges of tacora volcano (northern Chile). J Volcanol Geotherm Res 208:77–85

Cembrano J, Lara L (2009) The link between volcanism and tectonics in the southern volcanic zone of the Chilean Andes: A review. Tectonophysics 471:96–113

Chiodini G, Marini L (1998) Hydrothermal gas equilibria: the H_2O-H_2-CO_2-CO-CH_4 system. Geochim Cosmochim Acta 62:2673–2687

Chiodini G, Allard P, Caliro S, Parello F (2000) ^{18}O Exchange between steam and carbon dioxide in volcanic and hydrothermal gases: isotopic and genetic implications. Geochim Cosmochim Acta 64:2479–2488

Chiodini G, Marini L, Russo M (2001) Geochemical evidence for the existence of high-temperature hydrothermal brines at Vesuvio volcano, Italy. Geochim Cosmochim Acta 65:2129–2147

Christenson BW, Wood CP (1993) Evolution of a vent hosted hydrothermal system beneath Ruapehu crater, New Zealand. Bull Volcanol 55:547–565

Coleman ML, Shepherd TJ, Rouse JE, Moore GR (1982) Reduction of water with zinc for hydrogen isotope analysis. Anal Chem 54:993–995

Contreras-reyes E, Flueh ER, Grevemeyer I (2010) Tectonic control on sediment accretion and subduction off south-central Chile: implications for coseismic rupture processes of the 1960 and 2010 megathrust earthquakes. Tectonics 29:1–32

Craig H (1961) Isotopic variations in meteoric waters. Science 133:1702–1703

Craig H, Lupton JE (1976) Primordial neon, helium and hydrogen in oceanic basalts. Earth Planet Sci Lett 31:369–385

D'Amore F, Panichi C (1980) Evaluation of deep temperature of hydrothermal systems by a new gas-geothermometer. Geochim Cosmochim Acta 44:549–556

de Leeuw GMA, Hilton GA, Gulec DR, Mutlu N (2010) Regional and temporal variations in $CO_2/^3He$, $^3He/^4He$ and $d^{13}C$ along the north Anatolian fault zone, Turkey. Appl Geochem 25:524–539

Delmelle P, Bernard A, Kusakabe M, Fisher TP, Takano B (2000) Geochemistry of the magmatic-hydrothermal system of Kawah Ijen volcano, East Java, Indonesia. J Volcanol Geotherm Res 97:31–53

Domalski ES, Hearing ED (1993) Estimation of the thermodynamic properties of C–H–N–O–S–halogen compounds at 298.15 K. J Phys Chem Ref 22:805–1159

Epstein S, Mayeda TK (1953) Variation of the 18O/16O ratio in natural waters. Geochim Cosmochim Acta 4:213–224

Evans WC, White LD, Rapp JB (1998) Geochemistry of some gases in hydrothermal fluids from the southern Juan de Fuca ridge. J Geophys Res 15:305–313

Farley KA, Poreda RJ (1993) Mantle neon and atmospheric contamination. Earth Planet Sci Lett 114:325–339

Giambiagi LB, Ramos VA (2002) Structural evolution of the Andes in a transitional zone between flat and normal subduction (33 30′–33 45′S), Argentina and Chile. J South Am Earth Sci 15:101–116

Giggenbach WF (1975) A simple method for the collection and analysis of volcanic gas samples. Bull Volcanol 39:132–145

Giggenbach WF (1980) Geothermal gas equilibria. Geochim Cosmochim Acta 44:2021–2032

Giggenbach WF (1984) Mass transfer in hydrothermal alteration systems—a conceptual approach. Geochim Cosmochim Acta 48:2693–2711

Giggenbach WF (1987) Redox processes governing the chemistry of fumarolic gas discharges from white island, New Zealand. Appl Geochem 2:143–161

Giggenbach WF (1988) Geothermal solute equilibria, derivation of Na-K-Mg-Ca geoindicators. Geochim Cosmochim Acta 52:2749–2765

Giggenbach WF (1992a) Isotopic shifts in waters from geothermal and volcanic systems along margins, and their origin. Earth Planet Sci Lett 113:495–510

Giggenbach WF (1992b) The composition of gases in geothermal and volcanic systems as a function of tectonic setting. Proc Int Symp Water-Rock Interaction WRI-8:873–878

Giggenbach WF (1993) Redox control of gas compositions in Philippine volcanic–hydrothermal systems. Geothermics 22:575–587

Giggenbach WF (1996) Chemical composition of volcanic gases. In: Scarpa M, Tilling R (eds) Monitoring and mitigation of volcanic hazards. Springer, Berlin, pp 221–256

Giggenbach WF (1997) The origin and evolution of fluids in magmatic-hydrothermal systems. In: Barnes HL (ed) Geochemistry of hydrothermal ore deposits, 3rd edn. Wiley, New York, pp 737–796

González-ferrán O (1995) Volcanes de Chile. Instituto Geográfico Militar, Santiago, Chile, p 639

Grevemeyer I, Diaz-Naveas JL, Ranero CR, Villinger HW, Ocean Drilling Program Leg 202 Scientific Party (2003) Heat flow over the descending nazca plate in central Chile, 32°S to 41°S: observations from ODP Leg 202 and the occurrence of natural gas hydrates. Earth Planet Sci Lett 213:285–298

Hildreth W, Moorbath S (1988) Crustal contributions to arc magmatism in the Andes of central Chile. Contrib Mineral Petrol 98:455–489

Hilton DR, Fischer TP, Marty B (2002) Noble gases and volatile recycling at subduction zones. Rev Mineral Geochem 47:319–370

Horita J, Cole DR, Wesolowski DJ (1994) Liquid–vapor fractionation of oxygen and hydrogen isotopes of water from the freezing to the critical temperature. Geochim Cosmochim Acta 58:3425–3437

Inguaggiato S, Rizzo A (2004) Dissolved helium isotope ratios in groundwaters: a new technique based on gas–water re-equilibration and its application to Stromboli volcanic system. Appl Geochem 19:665–673

Jenden PD, Kaplan IR, Poreda RJ, Craig H (1988) Origin of nitrogen-rich gases in the californis great valley: evidence from helium, carbón and nitrogen isotope ratios. Geochim Cosmochim Acta 52:851–861

Jenden PD, Hilton DR, Kaplan IR, Craig H (1993) Abiogenic hydrocarbons and mantle helium in oil and gas fields. In: Howell DG (ed). The future of energy gases. US Geological Survey Professional Paper, 1570, pp. 31–56.

Jochum KP, Hokman AW, Ito E, Seufert HM, White WM (1983) K, U, and Th in mid-ocean ridge basalt glasses and heat production, K/U and K/Rb in the mantle. Nature 306:431–436

Lide DR (2001) Handbook of chemistry and physics, 82nd edn. CRC, Boca Raton, FL, USA

Mamyrin BA, Tolstikhin IN (1984) Helium isotopes in nature. In: Fyfe WS (ed) Development in geochemistry. Elsevier, Amsterdam, p 288

Martini M, Giannini L, Buccianti A, Prati F, Cellini-Le-gittimo P, Iozzelli P, Capaccioni B (1991) 1980–1990: ten years of geochemical investigation at Phlegrean Fields (Italy). J Volcanol Geotherm Res 48:161–171

Marty B (1995) Nitrogen content of the mantle inferred from N2–Ar correlation in oceanic basalts. Nature 377:326–329

Marty B, Jambon A (1987) $C/^3He$ in volatile fluxes from the solid earth—implications for carbon geodynamics. Earth Planet Sci Lett 83:16–26

Matsuo S, Suzuki J, Mitzutani Y (1978) Nitrogen to argon ratio in volcanic gases. In: Alexander EC, Ozima M (eds) Terrestrial rare gases. Japan Science Society Press, Tokyo, pp 17–25

Montegrossi G, Tassi F, Vaselli O, Buccianti A, Garofalo K (2001) Sulfur species in volcanic gases. Anal Chem 73:3709–3715

Mook WG, Bemmerson JC, Steverman WH (1974) Carbon isotope fractionation between dissolved bicarbonate and gaseous carbon dioxide. Earth Planet Sci Lett 22:169–176

Moreno H, Naranjo JA (1991) The southern Andes Volcanoes (33°–41° 30′S), Chile. 6th geol Cong Chile, Excur pc-3, pp. 26

Ohba T (2007) Formation process of recent fumarolic gases at the Mt. Mihara summit peak of the Izu-Oshima volcano, Japan. Earth Planets Space 59:1127–1133

Ohba T, Daita Y, Sawa T, Taira N, Kakuage Y (2011a) Coseismic changes in the chemical composition of volcanic gases from the Owakudani geothermal area on Hakone volcano, Japan. Bull Volcanol 73:457–469

Ohba T, Nogami K, Hirabayashi J, Sawa T, Kazahaya K, Morikawa N, Ohwada M (2011b) Chemical and isotopic composition of fumarolic gases at Iwate volcano, Japan, during and after seismic activity in 1998: implications for the modification of ascending volcanic gases. Ann Geophys 54(2):187–197

O'Nions R, Oxburgh E (1988) Helium, volatile fluxes and the development of continental crust. Earth Planet Sc Lett 90:331–347

Oremland RS, Miller LG, Whiticar MJ (1987) Sources and flux of natural gases from mono lake, California. Geochim Cosmochim Acta 51:2915–2929

Pasternack GB, Varekamp JC (1997) Volcanic lake systematics I. Physical constraints. Bull Volcanol 58:528–538

Poreda R, Craig H (1989) Helium isotope ratios in circum-pacific volcanic arcs. Nature 338:473–478

Ramos VA, Cristallini E, Introcaso A (2004) The Andean thrust system latitudinal variations in structural styles and orogenic shortening. AAPG Spec Vol Memoir 82: thrust tectonics and hydrocarbon systems, pp. 30–50

Ray M, Hilton D, Muñoz J, Fischer T, Shaw A (2009) The effects of volatile recycling, degassing and crustal contamination on the helium and carbon geochemistry of hydrothermal fluids from the southern volcanic zone of Chile. Chem Geol 266(1–2):38–49

Reid RC, Prausnitz JM, Poling BE (1987) The properties of gases and liquids. McGraw-Hill, New York, p 768

Sano Y, Marty B (1995) Origin of carbon in fumarolic gas from island arcs. Chem Geol 119:265–274

Sarda P, Moreira M (2002) Vesiculation and vesicle loss in mid-ocean ridge basalt glasses: He, Ne, Ar elemental fractionation and pressure influence. Geochim et Cosmochim Ac 66:1449–1458

Sarda P, Staudacher T, Allegre CJ (1985) $^{40}Ar/^{36}Ar$ In MORB glasses: constraints on atmosphere mantle evolution. Earth Planet Sci Lett 72:357–375

Schoell M (1980) The hydrogen and carbon isotopic composition of methane from natural gases of various origins. Geochim Cosmochim Acta 44:649–661

Schoell M (1988) Multiple origins of methane in the Earth. Chem Geol 71:1–10

Seewald JS (2001) Aqueous geochemistry of low molecular weight hydrocarbons at elevated temperatures and pressures: constraints from mineral buffered laboratory experiments. Geochim Cosmochim Acta 65:1641–1664

Sepúlveda F, Lahsen A, Powell T (2007) Gas geochemistry of the Cordón Caulle geothermal system, Southern Chile. Geothermics 36:389–420

Shinohara H, Hirabayashi J, Nogami K, Igushi M (2011) Evolution of volcanic gas composition during repeated culmination of volcanic activity at Kuchinoerabujima volcano, Japan. J Volcanol Geoth Res 202:107–116

Snyder G, Poreda R, Fehn U, Hunt A (2003) sources of nitrogen and methane in central american geothermal settings: noble gas and ^{129}i evidence for crustal and magmatic volatile components. Geochem Geophys Geosyst. doi:10.1029/2002gc000363

Stern C, Moreno H, López-Escobar L, Clavero J, Lara L, Naranjo J, Parada M, Skewes A (2007) Chilean volcanoes. In: Moreno T, Gibbons W (eds) Geology of Chile. Geol, Soc. London, pp 309–328

Stevenson S (1993) Physical models of fumarolic flow. J Volcanol Geotherm 57(3–4):139–156

Strand K (1995) Semmicrostructural analysis of a volcanogenic sediment component in a trench.slope basin of the Chile margin. In: Lewis SD, Behrmann JH, Musgrave RJ, Cande SC (eds). Proceedings of the Ocean Drilling Program, Scientific Results, 141, pp. 169–180.

Symonds R, Gerlach T, Reed M (2001) Magmatic gas scrubbing: implications for volcano monitoring. J Volcanol Geotherm Res 108:303–341

Taran YA, Giggenbach WF (2003) Geochemistry of light hydrocarbons in subduction related volcanic and hydrothermal fluids. Soc Econ Geol 10:61–74

Taran YA, Pokrovsky B, Esikov A (1989) Deuterium and oxygen-18 in fumarolic steam and amphiboles from some Kamchatka volcanoes: "Andesitic waters". Dokl Akad Nauk SSSR 304:440–443

Taran YA, Connor CB, Shapar VN, Ovsyannikov AA, Bilichenko AA (1997) Fumarolic activity of Avachinsky and Koryaksky volcanoes, Kamchetka, from 1993 to 1994. Bull Volcanol 58:441–448

Tassara A, Yáñez G (2003) Relación entre el espesor elástico de la litósfera y la segmentación tectónica del margen andino (15–47°S). Rev Geol Chile 32:159–186

Tassi F, Martinez C, Vaselli O, Capaccioni B, Viramonte J (2005a) Light hydrocarbons as redox and temperature indicators in the geothermal field of El tatio (northern Chile). Appl Geochem 20:2049–2062

Tassi F, Vaselli O, Capaccioni B, Giolito C, Duarte E, Fernandez E, Minissale A, Magro G (2005b) The hydrothermal–volcanic system of Rincon de la Vieja volcano (Costa Rica): a combined (inorganic and organic) geochemical approach to understanding the origin of the fluid discharges and its possible application to volcanic surveillance. J Volcanol Geotherm Res 148:315–333

Tassi F, Aguilera F, Vaselli O, Medina E, Tedesco D, Delgado Huertas A, Poreda R, Kojima S (2009a) The magmatic- and hydrothermal-dominated fumarolic system at the active crater of Lascar volcano, northern Chile. Bull Volcanol 71:171–183

Tassi F, Vaselli O, Fernandez E, Duarte E, Martinez M, Delgado Huertas A, Bergamaschi F (2009b) Morphological and geochemical features of crater lakes in Costa Rica: an overview. J Limnol 68(2):1–13

Tassi F, Montegrossi G, Capaccioni B, Vaselli O (2010) Origin and distribution of thiophenes and furans in thermal fluid discharges from active volcanoes and geothermal systems. Int J Mol Sci 11:1434–1457

Tassi F, Aguilera F, Vaselli O, Darrah T, Medina E (2011) Gas discharges from four remote volcanoes (Putana, Olca, Irruputuncu and Alitar) in northern Chile: a geochemical and isotopic survey. Ann Geophys 54:121–136

Tassi F, Fiebig J, Vaselli O, Nocentini M (2012) Origins of methane discharging from volcanic, hydrothermal and cold emissions in Italy. Chem Geol 310–311:36–48

Taylor BE (1986) Magmatic volatiles: isotopic variation of C, H and S. Rev Mineral 16:185–225

Tedesco D, Sabroux JC (1987) The determination of deep temperatures by means of the CO-CO_2-H_2-H_2O geothermometer: an example using fumaroles in the Campi Flegrei, Italy. Bull Volcanol 49:381–387

Varekamp JC, Pasternack GB, Rowe GL (2000) Volcanic lake systematics II. Chemical constraints. J Volcanol Geotherm Res 97:161–179

Varekamp JC, deMoor JM, Merrill MD, Colvin AS, Goss AR, Vroon PZ, Hilton DR (2006) Geochemistry and isotopic characteristics of the Caviahue-Copahue volcanic complex, Province of Neuquen, Argentina. Geol Soc Am 407:317–342

Vaselli O, Tassi F, Montegrossi G, Capaccioni B, Giannini L (2006) Sampling and analysis of fumarolic gases. Acta Vulcanol 18:65–76

Vaselli O, Tassi F, Duarte E, Fernandez E, Poreda RJ, Delgado Huertas A (2010) Evolution of fluid geochemistry at the turrialba volcano (Costa Rica) from 1998 to 2008. Bull Volcanol 72:397–410

von Huene R, Scholl DW (1991) Observations at convergent margins concerning sediment subduction, subduction erosion, and the growth of continental crust. Rev Geophys 29:279–316

Whiticar MJ, Suess E (1990) Hydrothermal hydrocarbon gases in the sediments of the King George basin, Bransfield Strait, Antarctica. Appl Geochem 5:135–147

Whiticar MJ (1999) Carbon and hydrogen isotope systematics of bacterial formation and oxidation of methane. Chem Geol 161:291–314

Zelenski M, Taran Y (2011) Geochemistry of volcanic and hydrothermal gases of Mutnovsky volcano, Kamchactka: evidence for mantle, slab and atmosphere contributions to fluids of a typical arc volcano. Bull Volcanol 73:373–394